Zoosyst. Evol. 99 (2) 2023, 391–397 | DOI 10.3897/zse.99.105770

First report of a histozoic *Henneguya* (Cnidaria, Endocnidozoa) infecting a synbranchid potamodromous fish from South America: Morphostructural and biological data

Patrick D. Mathews[1,2], Omar Mertins[2], Luis L. Espinoza[3], Julio C. Aguiar[1], Tiago Milanin[4]

1 *Department of Parasitology, Institute of Biosciences, São Paulo State University, 18618-689 Botucatu, Brazil*
2 *Laboratory of Nano Bio Materials, Department of Biophysics, Paulista Medical School, Federal University of Sao Paulo, 04023-062 São Paulo, Brazil*
3 *Laboratory of Biology and Molecular Genetics, Faculty of Veterinary Medicine, Universidad Nacional Mayor de San Marcos, Lima 15021, Peru*
4 *Department of Basic Sciences, Faculty of Animal Science and Food Technology, University of São Paulo, 13635-900, Pirassununga, Brazil*

https://zoobank.org/7D9E1775-A6FC-49D0-9B89-EBF51D3DC912

Corresponding author: Patrick D. Mathews (patrickmathews83@gmail.com)

Academic editor: Pavel Stoev ♦ **Received** 1 May 2023 ♦ **Accepted** 12 June 2023 ♦ **Published** 5 July 2023

Abstract

In this study, a *Henneguya* myxosporean species is described to infect an ecological, biological, and evolutionary important fish from Amazon biome. The myxosporean was found in the skin of only one specimen of marbled swamp eel, *Synbranchus marmoratus* caught in a small stream from Peruvian Amazon floodplain. Mature myxospores have ovoid shape from the valvular view, measuring 32.2 ± 0.6 µm (31.6–32.8) in total length, 21.5 ± 0.3 µm (21.2–21.8) in spore body length, 11.7 ± 0.5 µm (11.2–12.2) in width and 10.6 ± 0.9 µm (9.7–11.5) in thickness. Non-bifurcate caudal appendage, measuring 10.7 ± 0.4 µm (10.3–11.1) in length. Two polar capsules elongated aubergine in shape, equal in size and measuring 4.9 ± 0.2 µm (4.7–5.1) in length and 3.1 ± 0.5 µm (2.6–3.6) in width. Polar tubules coiled in 7–8 turns. This is the first report of a *Henneguya* species parasitizing a fish of the order Synbranchiformes from Amazon basin and the first to describe this parasite infecting a potamodromous fish from South America.

Key Words

Henneguya, myxosporean, marbled swamp eel, skin, Peru

Introduction

Myxosporean are a biologically diverse group of microscopic cnidarians of wide distribution around the world (Atkinson et al. 2018). They mostly innocuous parasites with complex life cycles that involve invertebrate and vertebrate hosts (Okamura et al. 2015). Although, most myxosporean species have fish hosts, they have radiated sporadically into other groups of vertebrates, including amphibians, reptiles, waterfowl and small mammals (Okamura et al. 2015). Within myxosporean, *Henneguya* Thélohan, 1892 is one of the most species rich genera with more than 250 species described taxonomically (Eiras 2002; Rangel et al. 2023). Although the Amazon basin is one of the main biodiversity hotspots, the myxosporean fauna is poorly known. To date only 19 *Henneguya* species have been reported in fish from this geographic region with almost all reported data so far coming from the Brazilian part of the Amazon basin (Eiras and Adriano 2012; Mathews et al. 2016; Naldoni et al. 2018). In the Peruvian Amazon, despite a recording of over 650 fish species, there is a gap in the knowledge of myxosporean diversity. Indeed, only three *Henneguya* species have been described (Mathews et al. 2017, 2018, 2020).

The marbled swamp eel *Synbranchus marmoratus* Bloch, 1795 is considered a potential predator and it can be found throughout flooded forests, small streams and associated swamps subject to water level changes, between the rainy season and the dry period (Heisler 1982; Favorito et al. 2005;

Junges et al. 2010). This species of fish is a protogynous diandric, meaning that females will change their sex and become males (Allsop and West 2003). It is a potamodromous species which is capable of switching from exclusive water breathing to exclusive air breathing (Heisler 1982). Despite, the ecological, biological, and evolutive importance of the marbled swamp eel, little is known about its parasitic fauna, particularly the ones concerning myxosporean parasites.

This study aims to contribute to the increase of knowledge of diversity cnidarian myxosporean and their interaction with fishes from Amazon biome. Thus, spore morphology features using light, scanning and transmission electron microscopy as well as other important biological characters such as tissue tropism and host-specificity are provided.

Materials and methods

Six specimens of *S. marmoratus* (ranging from 18.1 to 21.6 cm in length) that died during transport were donated by local fishers for ornamental fishes in March 2018. According to the fishers, these fish were caught in a small stream near of the Village Oran (3°21'0"S, 72°31'0"W), Omagua Region, Department of Loreto, Peru.

Morphometric analysis was performed following the criteria outlined by Lom and Arthur (1989). Measurements and photographs were taken from 30 randomly selected formalin-fixed mature myxospores, using a computer equipped with Axiovision 4.1 image capture software coupled to an Axioplan 2 Zeiss microscope (Carl Zeiss AG, Oberkochen, Germany). Spore length, thickness, polar capsule length, width, and caudal appendage length were measured and given in micrometers (µm) and expressed as a mean ± standard deviation, followed by the range in parentheses where appropriate. Permanent slides containing mature myxospores stained with Giemsa were mounted and deposited in the cnidarian collection of the Zoology Museum at the University of São Paulo – MZUSP, São Paulo, Brazil (Hapantotype MZUSP 8733).

Histological analysis was performed on fresh tissue fragments containing plasmodium. Infected tissue was fixed in 10% buffered formalin solution, then dehydrated with increasing series of ethanol, diaphanized, embedded in paraffin, cut into serial sections 5 µm thick using an HM 340E electron microtome (Thermo ScientificTM, Massachusetts, USA), and stained with haematoxylin/eosin. A light microscope DM1000 (Leica, Washington, USA) coupled to a computer and using the Leica Application Suite software version 1.6.0 was used for image capture.

Surface ultrastructure observation was performed in leaked myxospores from ruptured plasmodium using a glass slide previously treated with poly-L-lysine. Samples were processed as described in Mathews et al. (2022a). Samples were visualized with a DSM 940 scanning electron microscope (Carl Zeiss, Hamburg, Germany) operating at 15 kV. For internal structural analyses, a whole intact plasmodium was fixed in 2.5% glutaraldehyde with 0.1 M buffered cacodylate (pH 7.4) for 24 h and processed routinely according to standard transmission electron microscope methods. Samples were examined under a JEOL 1200 EX II transmission electron microscope at 60 kV and micrographs were captured with a GATAN 791 camera.

For molecular diagnostic, extraction of genomic DNA (gDNA) was performed in a single plasmodium dissected from the skin and fixed in absolute ethanol. The gDNA was extracted using a DNeasy Blood & Tissue Kit (Qiagen Inc., California, USA), in accordance with the manufacturer's instructions for animal tissue protocol. Polymerase chain reactions (PCRs) were conducted in a final volume reaction of 25 µL, which comprised 10–50 ng of extracted DNA, 0.2 pmol for each primer, 12.5 µL of Dream Taq Green PCR Master Mix (Thermo Scientific) and nuclease-free water. Partial 18S rDNA sequence was amplified using routinely chosen primers paired as follows ERIB1 with ACT1r and Myxgen4F with ERIB10 (Barta et al. 1997, Kent et al. 2000, Hallett and Diamant 2001). PCRs were performed in an AG22331 Hamburg Thermocycler (Eppendorf, Hamburg, Germany) and amplification thermal cycling consisted of 95 °C for 5 min, followed by 35 cycles at 95 °C for 1 min, 58 °C for 1 min, 72 °C for 2 min, and then final elongation at 72 °C for 5 min. Amplification PCR products were electrophoresed in 2.0% agarose gel in a Tris-Acetate EDTA buffer, stained with Sybr Safe DNA gel stain (Invitrogen by Life Technologies, Carlsbad, USA), and analyzed under a Stratagene 2020E trans illuminator (Stratagene California, San Diego, USA). Band sizes of the amplicons was estimated by comparison with the concurrently run molecular weight marker 1 Kb Plus DNA Ladder (Invitrogen by Life Technologies). PCR products were purified using USB ExoSap-IT (Thermo Fisher Scientific, Waltham, USA) in accordance to the manufacturer's instructions. Purified PCR amplicons were sequenced using the same PCR primers and performed with a BigDye Terminator v3.1 cycle sequencing kit (Applied Biosystems Inc., California, USA) in an ABI 3730 DNA sequencing analyzer.

Results

Of six wild specimens of *S. marmoratus*, a single wild specimens of *S. marmoratus* examined, was infected in the skin by an unknown cnidarian myxosporean species. Based on the phenotypic characters of the mature myxospores, this species was assigned to the genus *Henneguya*. The fish presented five plasmodia distributed in the body skin. The same were not found in any other organ.

Taxonomic summary

Phylum: Cnidaria Verrill, 1865.
Subphylum: Endocnidozoa Schuchert, 1996.
Class: Myxosporea Bütschli, 1881.
Order: Bivalvulida Shulman, 1959.
Family: Myxobolidae Thélohan, 1892.

Genus *Henneguya* Thélohan, 1892

Species. *Henneguya* sp. (We suggest that this isolate, after determination by molecular phylogenetic data, be named as (*H. atingae*) based on host species common name in Peru.

Type host. *Symbranchus marmoratus* (Teleostei: Symbranchidae).

Site of infection. Stratus corneum of epidermis layer of the skin.

Type locality. Small stream, adjacent area of Oran Village, Loreto Department, Peru (3°21'0"S, 72°31'0"W).

Description. Morphological observations by light microscopic showed mature myxospores have ovoid shape from the valvular view, measuring 32.2 ± 0.6 µm (31.6–32.8) in total length, 21.5 ± 0.3 µm (21.2–21.8) in spore body length, 11.7 ± 0.5 µm (11.2–12.2) in width and 10.6 ± 0.9 µm (9.7–11.5) in thickness (Fig. 1a, c). Non-bifurcate caudal appendage, measuring 10.7 ± 0.4 µm (10.3–11.1) in length (Fig. 1a, c). Two polar capsules elongated aubergine in shape, equal in size and measuring 4.9 ± 0.2 µm (4.7–5.1) in length and 3.1 ± 0.5 µm (2.6–3.6) in width (Fig. 1b, c). Sporoplasm evidenced two nuclei in valvular view and sutural line was noticeable in side view (Fig. 1b, c).

Surface topography analyses of mature myxospores in valvular view revealed smooth valve cell with presence of mucous in a small area (Fig. 2a). In sutural view myxospore evidence a conspicuous sutural line (Fig. 2c). The density of caudal appendage is likely be identical to that of its valve (Fig. 2b). Internal ultrastructural observations showed binucleated sporoplasm contained sev-

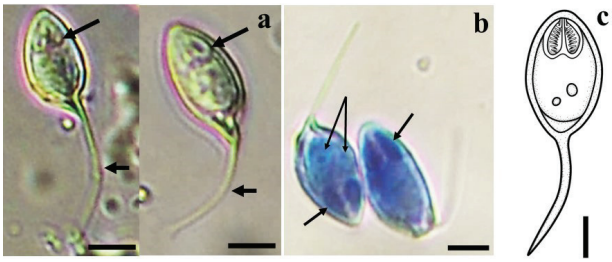

Figure 1. *Henneguya* sp. parasite from the skin of *Synbranchus marmoratus*. **a**: formalin-fixed myxospores in valvular view showing appendage caudal (large arrows) and two polar capsules in the anterior pole of spore occupied only the anterior third of the myxospore body (small blue arrows). **b**: mature myxospores stained with Giemsa with noticeable binucleate sporoplasm (double arrow) and polar capsules with aubergine shape (large arrow). **c**: schematic illustration of mature myxospore with polar tubule inside of polar capsule. Scale bars: 5 µm.

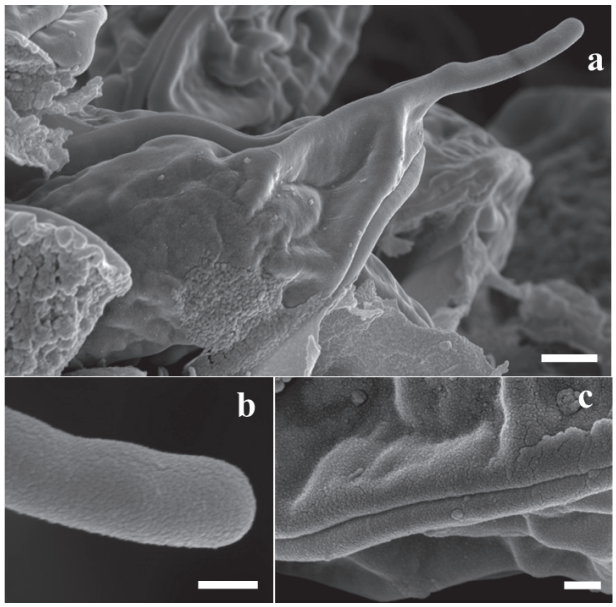

Figure 2. Surface topography by SEM of *Henneguya* sp. infecting skin of *Synbranchus marmoratus*. **a**: mature myxospore in valvular view showing smooth valve cell with presence of mucous (white star) in a small area and caudal appendage. Scale bar. 1 µm. **b**: amplified area of the caudal appendage evidencing density of caudal appendage likely to be identical to that of its valve. Scale bar. 200 nm **c**: myxospore evidence a conspicuous sutural line in sutural view. Scale bar: 100 nm.

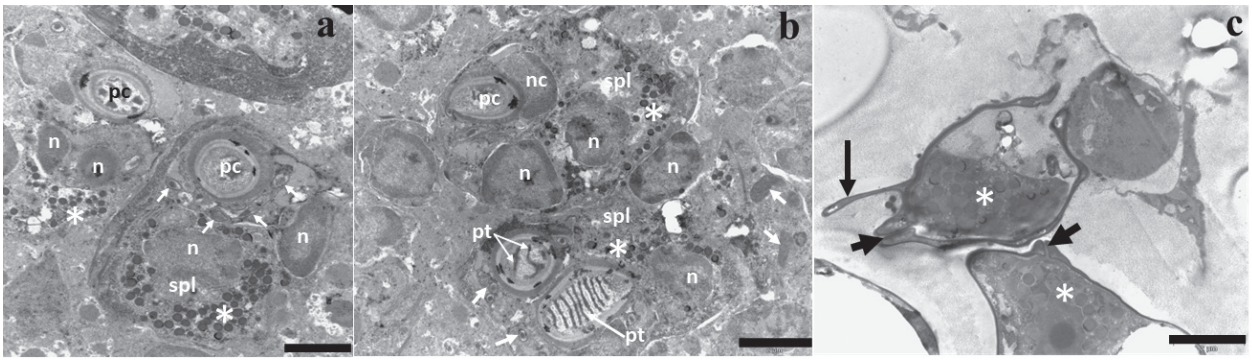

Figure 3. Internal ultrastructure by TEM of myxospore of *Henneguya* sp. infecting skin of *Synbranchus marmoratus*. **a**: sporoblast in young developmental stage showing binucleated sporoplasm (n) contained several sporoplasmosomes (asterisk), valve-forming materials (white arrow) and polar capsules (pc) with absence of polar tubule. **b**: polar capsule (pc) with capsular nuclei, polar tubule internalized contained seven to eight coils (pt), sporoplasm binucleated (spl/n) and contained sporoplasmosomes (asterisk) at a more advanced sporoblast developmental stage. **c**: Spores with sutural lines (small arrows), sporoplasm with numerous sporoplasmosomes (asterisk) and caudal appendage (large arrow). Scale bars: 2 µm.

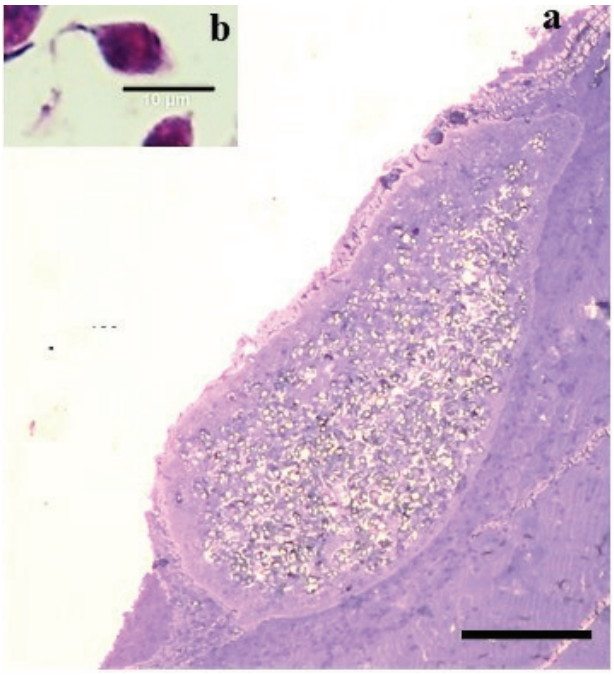

Figure 4. Histological sections of the host-tissue infected of *Synbranchus marmoratus* with *Henneguya* sp. **a**: Intact plasmodium located in the stratus corneum of epidermis layer of the skin. Scale bar. 50 µm. **b**: mature myxospore in sutural view with noticeable caudal appendage. Scale bar. 10 µm.

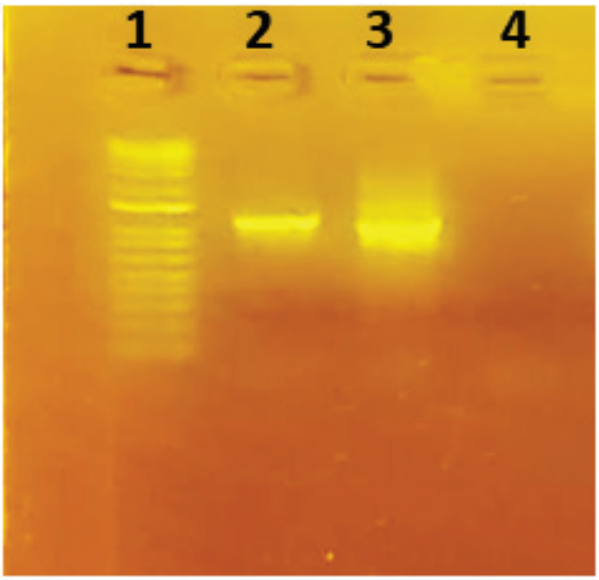

Figure 5. Agarose gel showing 18S rDNA gene PCR amplification of *Henneguya* sp. from skin infected of *S. marmoratus*. Lane 1: DNA ladder marker, Lane 2: amplicon 1000 pb approx. (ERIB1/ACT1r), Lane 3: amplicon 1100 pb approx. (Myxgen4F/ ERIB10), Lane 4: Negative Control.

eral sporoplasmosomes and valve-forming materials in young sporoblast developmental myxospore stage (Fig. 3a). Polar capsule with polar tubule internalized and contained seven to eight coils at a more advanced sporoblast developmental stage (Fig. 3b). Caudal appendage and conspicuous sutural line in mature spores. (Fig. 3c).

Histologic evidenced tissue tropism of the myxosporean under study, occurring in the stratus corneum of epidermis layer of the skin (Figure 4). The parasites induced no apparent tissue destruction, ulcerations, necrosis or inflammatory response. For molecular procedures, partial 18S rDNA gene was successfully amplified by PCR (Fig. 5), however, sequencing failed.

Discussion

Despite the growing description of myxosporean infecting South American fishes (Sousa et al. 2021; Adriano and Oliveira 2022), the diversity of these ancient metazoans in this neotropical realm remains largely unknown (Okamura et al. 2018; Mathews et al. 2022b). In this context, our study describes a histozoic myxosporean species of *Henneguya*, infecting skin of the Amazonian potamodromous fish *S. marmoratus*. In the Amazon biome, *Henneguya* encompasses 22 recognized species (Table 1), reported infecting Characiform, Perciform, Cichliform, Gymnotiform and Siluriform fishes (Mathews et al. 2017, 2018; Adriano and Oliveira 2022; Rangel et al. 2023). However, to the best of our knowledge, this is the first report of a *Henneguya* species parasitizing a fish of the order Synbranchiformes from Amazon basin and the first to describe this parasite infecting a potamodromous fish from South America. Thus, our results contribute to freshwater myxobolids taxonomy and to increasing our knowledge of cnidarian myxosporean diversity.

The morphological data of the mature myxospore isolated were first compared considering *Henneguya* species previously described from Peruvian Amazon freshwater fishes. Nevertheless, these differ from the new isolated in myxospore body length (18.7 ± 0.9 µm in length for *H. multiradiatus*, 14.3 ± 0.1 µm for *H. loretoensis*, 13.4 ± 0.9 µm for *H. peruviensis* and 21.5 ± 0.3 µm to the new isolated), polar capsule length (9.1 ± 0.1 µm in *H. multiradiatus*, 5.1 ± 0.2 µm in *H. loretoensis*, 3.3 ± 0.2 µm in *H. peruviensis* and 4.9 ± 0.2 µm in the new isolated), number of coils of the polar tubule (10–11 in *H. multiradiatus*, five in *H. loretoensis*, four to five in *H. peruviensis* and seven to eight in the new isolated) and in the length of the caudal appendage (25.8 ± 0.6 µm in *H. multiradiatus*, 21.9 ± 0.1µm in *H. loretoensis*, 10.7 ± 0.1 in *H. peruviensis* and 10.7 ± 1.2 µm in the new isolated). Compared with the all other freshwater *Henneguya* species reported to infect Amazonian fishes, the new isolated differed in at least one characteristic (shape of spore, size of spore or polar capsule, presence or absence or number of valve striations, size of caudal appendage and number of polar tubules turns), tissue and host preference as showed in the Table 1.

According to Molnár and Eszterbauer (2015), for freshwater histozoic myxosporean particularly for *Henneguya* and *Myxobolus* species, the site of infection is considered an important taxonomic key for identification due to high organ and/or tissue specificity of these group of parasites. Accordingly, differences are observed because plasmodia

Table 1. Comparative data of *Henneguya* sp. with other *Henneguya* species parasites of Amazon fish. Spore dimensions, infection sites, and fish host are given. TL: total length; BL: body length; APCL: caudal appendage length; SW: spore width; ST: spore thickness; PCL: polar capsule length; PCW: polar capsule width; NCT: number of coils of polar tubules, *: Peru. All measurements are in µm and/or means ± SD. Source: Rangel et al. 2023, Eiras, 2002.

Species	TL	BL	APCL	SW	ST	PCL	PCW	NCT	Site of infection	Fish species
**Henneguya sp.*	32.2 ± 0.6	21.5 ± 0.3	10.7 ± 0.4	11.7 ± 0.5	10.6 ± 0.9	4.9 ± 0.2	3.1 ± 0.5	7–8	skin	*Synbranchus marmoratus*
Henneguya longisporoplasma	53.4 ± 2.9	12.6 ± 0.6	40.7 ± 2.8	5.7 ± 0.5	5.3 ± 0.5	3.5 ± 0.3	1.9 ± 0.2	4–5	gill filaments, fins	*Plagioscion squamosissimus*
**Henneguya multiradiatus*	44.5 ± 0.6	18.7 ± 0.9	25.8 ± 0.6	7.1 ± 0.2	5.5 ± 0.3	9.1 ± 0.1	1.7 ± 0.1	10–11	Abdominal cavity serosa	*Brochis multiradiatus*
**Henneguya peruviensis*	24.2 ± 1.3	13.4 ± 0.9	10.7 ± 1.2	3.9 ± 0.1	–	3.3 ± 0.2	1.6 ± 0.2	4–5	Gill filaments	*Hyphessobrycon loretoensis*
**Henneguya loretoensis*	36. 2 ± 0.2	14.3 ± 0.1	21.9 ± 0.1	5.1 ± 0.2	–	5.1 ± 0.2	2.4 ± 0.3	5	Gill filaments	*Corydoras leucomelas*
Henneguya tucunarei	43.8 ± 4.1	14 ± 0.8	28.1 ± 4.3	6.1 ± 0.7	–	3.4 ± 0.5	1.98 ± 0.3	3–4	Gill filaments	*Cichla monoculus*
Henneguya tapajoensis	54.6 ± 3.9	16.4 ± 1.2	39 ± 3.9	7 ± 0.4	5 ± 0.1	4.2 ± 0.5	2.1 ± 0.4	4–5	Gill filaments	*Cichla pinima*
Henneguya jariensis	46.7 ± 1.5	13.4 ± 0.7	33.1 ± 1.7	6.5 ± 0.5	–	4 ± 0.3	2 ± 0.1	4	Fins	*Cichla monoculus*
Henneguya paraensis	42.3 ± 0.3	12.8 ± 0.42	29.5 ± 0.73	8.6 ± 0.3	–	7.4 ± 0.1	2.6 ± 0.1	5–7	Gill filaments	*Cichla temensis*
Henneguya melini	40.8 ± 0.3	15.5 ± 0.2	25.3 ± 0.1	4.7 ± 0.1	–	4.8 ± 0.5	1.7 ± 0.3	5–6	Gill filaments	*Corydoras melini*
Henneguya aequidens	41 ± 1.5	15 ± 0.9	27 ± 0.6	6 ± 0.8	–	3 ± 0.3	3 ± 0.3	4–6	Gill filaments	*Aequidens plagiozonatus*
Henneguya torpedo	48.62 ±0.5	28.53 ± 0.3	19.64 ±0.4	7.25 ± 0.31	3.06 ± 0.2	6.41 ± 0.2	1.84 ± 0.1	5–6	Brain and spinal cord	*Brachyhypopomus pinnicaudatus*
Henneguya arapaima	51.6 ± 3.4	14.2 ± 0.8	38.3 ± 2.9	5.7 ± 0.5	4.9 ± 0.2	6.5 ± 0.2	6.3 ± 0.1	5	Gill arch	*Arapaima gigas*
Henneguya rondoni	17.7	7	10.7	3.6	2.5	2.5	0.85	6–7	Lateral nerves	*Gymnorhamphichthys rondoni*
Henneguya rhamdia	50 ± 1.8	13.1 ± 1.1	36.9 ± 1.6	5.2 ± 0.5	–	4.7 ± 0.4	1.1 ± 0.2	10–11	Gill filaments	*Rhamdia quelen*
Henneguya schtzodon	28.9	13.1	16.3	3.3	–	5.4	1.3	8–10	Kidney	*Schtzodon fasciatum*
Henneguya friderici	33.8	10.4	23.3	5.7	4.9	4.9	2.1	7–8	Gut, gill, kidney and liver	*Leporinus friderici*
Henneguya astyanax	47.8 ± 0.71	15.2 ± 0.77	32.6 ± 1.11	5.7 ± 0.71	4.2 ± 0.3	5.0 ± 0.13	1.5 ± 0.07	8–9	Gill filaments	*Astyanax bimaculatus*
Henneguya curimata	35.4	16.6	19.1	6.2	–	3.3 ± 0.02	1.5 ± 0.04	10–11	Kidney	*Curimata inormata*
Henneguya testicularis	27.5	14	13.5	6.5	–	9	2	12–13	Testicle	*Moenkhausia oligolepis*
Henneguya malabarica	28.3	12.6	17.1	4.8	–	3.7	1.8	6–7	Gill filaments	*Hoplias malabaricus*
Henneguya adherens	32.3	12.4	20.5	5.8	–	3.1	1.2	3–4	Gill filaments	*Acestrorhynchus falcatus*
Henneguya amazonica	59.3 ± 0.5	13.9 ± 0.1	45.4 ± 0.6	5.7 ± 0.06	–	3.3 ± 0.02	1.5 ± 0.04	6	Gill lamellae	*Crenlcichla lepldota*

of the new species were located in the skin, whereas *H. peruviensis* and *H. loretoensis* plasmodia are found in the gill filaments and *H. multiradiatus* plasmodia in the abdominal cavity serosa. To our knowledge no *Henneguya* species have been reported from the skin of a fish from Amazon biome (Table 1). In the same vein, fish host represent an indispensable trait for accurately distinguishing new freshwater histozoic *Henneguya*/*Myxobolus* species since these parasites tend to cluster largely based on host phylogenies (Carriero et al. 2013; Mathews et al. 2021; Milanin et al. 2021). This is the first report of a *Henneguya* species parasitizing a synbranchid fish. Thus, considering the fine-scale of the host-specificity, we consider our finding to be important for this isolate as an unknown species.

Regarding molecular data, from South America of the around hundred recognized species, large number of species lack molecular data (Milanin et al. 2017). Indeed, for much of the myxosporean described myxospore morphology was used by ichthyopathologist researchers for species discrimination, because myxo-

spore is a unique structure possessing many characters important for classification (Lom and Dyková 1992). In our study, the partial 18S rDNA gene was successfully amplified by PCR using general eukaryotic and specific primers to myxosporean parasites (Fig. 5). However, after the amplification process, sequencing failed so it was not possible to carry out phylogenetic analysis. In addition, to the few samples with only five plasmodia to perform morphological, ultrastructural, histological and molecular analysis and limitations in accessing new samples of the same region. Although, we were not able to provide the phylogenetic data, the new isolate was strongly characterized based on spore morphometrically features as well as biological traits such as tissue preference and host specificity both important taxonomic keys for classification of freshwater histozoic myxobolids. Future molecular phylogenetic studies are highly recommended, since this would permit stronger taxonomic comparison.

Acknowledgements

The authors thank the São Paulo Research Foundation, FAPESP, for Post-Doc fellowship awarded to P.D. Mathews. The authors are grateful to A.H. Aguillera, P.A. Cortez and Prof. R. Sinigaglia-Coimbra from the Electron Microscopy Center (CEME) at UNIFESP for supporting the SEM and TEM analysis. The authors thank Dr. Christopher George Berger from Occidental College, Los Angeles for revision of the English language.

References

Adriano EA, Oliveira OMP (2022) Myxobolidae in Catálogo Taxonômico da Fauna do Brasil. PNUD. http://fauna.jbrj.gov.br/fauna/faunadobrasil/152860 [Accessed 18 Jan 2022]

Allsop DJ, West SA (2003) Constant relative age and size at sex change for sequentially hermaphroditic fish. Journal of Evolutionary Biology 16(5): 921–929. https://doi.org/10.1046/j.1420-9101.2003.00590.x

Atkinson SD, Bartholomew JL, Lotan T (2018) Myxozoans: Ancient metazoan parasites find a home in phylum Cnidaria. Zoology (Jena, Germany) 129: 66–68. https://doi.org/10.1016/j.zool.2018.06.005

Barta JR, Martin DS, Liberator PA, Dashkevicz M, Anderson JW, Feighner SD, Elbrecht A, Perkins-Barrow A, Jenkins MC, Danforth D, Ruff MD, Profous-Juchelka H (1997) Phylogenetic relationships among eight *Eimeria* species infecting domestic fowl inferred using complete small subunit ribosomal DNA sequences. The Journal of Parasitology 83(2): 262–271. https://doi.org/10.2307/3284453

Carriero MM, Adriano EA, Silva MRM, Ceccarelli PS, Maia AAM (2013) Molecular phylogeny of the *Myxobolus* and *Henneguya* genera with several new South American species. PLoS ONE 8: e73713. https://doi.org/10.1371/journal.pone.0073713

Eiras JC (2002) Synopsis of the species of the genus *Henneguya* Thelohan, 1892 (Myxozoa: Myxosporea: Myxobolidae. Systematic Parasitology 52(1): 43–54. https://doi.org/10.1023/A:1015016312195

Eiras JC, Adriano EA (2012) Checklist of the species of the genus *Henneguya* Thélohan, 1892 (Myxozoa, Myxosporea, Myxobolidae) described between 2002 and 2012. Systematic Parasitology 83(2): 95–104. https://doi.org/10.1007/s11230-012-9374-7

Favorito SE, Zanata AM, Assumpção MI (2005) A new *Synbranchus* (Teleostei: Synjbranchidae) from Ilha de Marajó, Pará, Brazil, with notes on its reproductive biology and larval development. Neotropical Ichthyology 3: 319–328. https://doi.org/10.1590/S1679-62252005000300001

Hallett SL, Diamant A (2001) Ultrastructure and small-subunit ribosomal DNA sequence of *Henneguya lesteri* n. sp. (Myxosporea), a parasite of sand whiting *Sillago analis* (Sillaginidae) from the coast of Queensland, Australia. Diseases of Aquatic Organisms 46: 197–212. https://doi.org/10.3354/dao046197

Heisler N (1982) Intracellular and extracellular acid-base regulation in the tropical fresh-water teleost fish *Synbranchus marmoratus* in response to the transition from water breathing to air breathing. The Journal of Experimental Biology 99(1): 9–28. https://doi.org/10.1242/jeb.99.1.9

Junges CM, Lajmanovich RC, Peltzer PM, Attademo AM, Bassó A (2010) Interactions between *Synbranchus marmoratus* (Teleostei: Synbranchidae) and *Hypsiboas pulchellus* tadpoles (Amphibia: Hylidae): importance of lateral line in nocturnal predation and effects of fenitrothion exposure. Chemosphere 81(10): 1233–1238. https://doi.org/10.1016/j.chemosphere.2010.09.035

Kent ML, Khattra J, Hedrick RP, Devlin RH (2000) *Tetracapsula renicola* n. sp. (Myxozoa: Saccosporidae); the PKX myxozoan: the cause of proliferative kidney disease of salmonid fishes. The Journal of Parasitology 86: 103–111. https://doi.org/10.1645/0022-3395(2000)086[0103:TRNSMS]2.0.CO;2

Lom J, Arthur JR (1989) A guideline for the preparation of species descriptions in Myxosporea. Journal of Fish Diseases 12(2): 151–156. https://doi.org/10.1111/j.1365-2761.1989.tb00287.x

Lom J, Dyková I (1992) Myxosporidia (Phylum Myxozoa). In: Lom J, Dyková I (Eds) Protozoan parasites of fishes. Developments in aquaculture and fisheries sciences Elsevier, Amsterdam, 159–235.

Mathews PD, Maia AAM, Adriano EA (2016) *Henneguya melini* n. sp. (Myxosporea: myxobolidae), a parasite of *Corydoras melini* (Teleostei: siluriformes) in the Amazon region: morphological and ultrastructural aspects. Parasitology Research 115(9): 3599–3604. https://doi.org/10.1007/s00436-016-5125-z

Mathews PD, Naldoni J, Adriano EA (2017) Morphology and small subunit rDNA- based phylogeny of a new *Henneguya* species, infecting the ornamental fish *Corydoras leucomelas* from the Peruvian Amazon. Acta Tropica 176: 51–57. https://doi.org/10.1016/j.actatropica.2017.07.017

Mathews PD, Mertins O, Pereira JOL, Maia AAM, Adriano EA (2018) Morphology and 18S rDNA sequencing of *Henneguya peruviensis* n. sp. (Cnidaria: Myxosporea), a parasite of the Amazonian ornamental fish *Hyphessobrycon loretoensis* from Peru: A myxosporean dispersal approach. Acta Tropica 187: 207–213. https://doi.org/10.1016/j.actatropica.2018.08.012

Mathews PM, Mertins O, Milanin T, Espinoza LL, Alama-Bermejo G, Audebert F, Morandini AC (2020) Taxonomy and 18S rDNA-based phylogeny of *Henneguya multiradiatus* n. sp. (Cnidaria: Myxobolidae) a parasite of *Brochis multiradiatus* from Peruvian Amazon. Microbial Pathogenesis 147: 104372. https://doi.org/10.1016/j.micpath.2020.104372

Mathews PD, Bonillo C, Rabet, N, Lord C, Causse R, Keith P, Audebert F (2021) Phylogenetic analysis and characterization of a new parasitic cnidarian (Myxosporea: Myxobolidae) parasitizing skin of the giant mottled eel from the Solomon Islands. Infection Genetics and Evolution 94: 104986. https://doi.org/10.1016/j.meegid.2021.104986

Mathews PD, Mertins O, Milanin T, Aguiar JC, Gonzales-Flores APP, Tavares LER, Morandini AC (2022a) Ultrastructure, surface topography, morphology and histological observations of a new parasitic cnidarian of the marbled swamp eel from the world's largest tropical wetland area, Pantanal, Brazil. Tissue & Cell 79: 101909. https://doi.org/10.1016/j.tice.2022.101909

Mathews PD, Mertins O, Flores-Gonzales APP, Espinoza LL, Aguiar JC, Milanin T (2022b) Host–Parasite Interaction and Phylogenetic of a new Cnidarian myxosporean (Endocnidozoa: Myxobolidae) Infecting a valuative commercialized ornamental fish from Pantanal wetland biome, Brazil. Pathogens (Basel, Switzerland) 11(10): 1119. https://doi.org/10.3390/pathogens11101119

Milanin T, Atkinson SD, Silva MR, Alves RG, Maia AA, Adriano EA (2017) Occurrence of two novel actinospore types (Cnidaria: Myxosporea) in Brazilian fish farms, and the creation of a novel actinospore collective group. Seisactinomyxon. Acta Parasitologica 62(1): 121–128. https://doi.org/10.1515/ap-2017-0014

Milanin T, Mathews PD, Morandini AC, Mertins O, Audebert F, Pereira JOL, Maia AA M (2021) Morphostructural data and phylogenetic relationships of a new cnidarian myxosporean infecting spleen of an economic and ecological important bryconid fish from Brazil. Microbial Pathogenesis 150: 104718. https://doi.org/10.1016/j.micpath.2020.104718

Molnár K, Eszterbauer E (2015) Specificity of Infection Sites in Vertebrate Hosts. In: Okamura B, Gruhl A, Bartholomew JL (Eds) Myxozoan Evolution, Ecology and Development. Springer, Switzerland, 295–313. https://doi.org/10.1007/978-3-319-14753-6_16

Naldoni J, Maia AAM, Correa LL, Da Silva MRM, Adriano EA (2018) New myxosporeans parasitizing *Phractocephalus hemioliopterus* from Brazil: Morphology, ultrastructure and SSU-rDNA sequencing. Diseases of Aquatic Organisms 128(1): 37–49. https://doi.org/10.3354/dao03210

Okamura B, Gruhl A, Bartholomew JL (2015) An introduction to Myxozoan evolution, ecology and development. In: Okamura B, Gruhl A, Bartholomew JL (Eds) Myxozoan Evolution, Ecology and Development, Springer, Switzerland, 1–20. https://doi.org/10.3354/dao03210

Okamura B, Hartigan A, Naldoni J (2018) Extensive uncharted biodiversity: The parasite dimension. Integrative and Comparative Biology 58: 1132–1145. https://doi.org/10.1093/icb/icy039

Rangel LF, Santos MJ, Rocha S (2023) Synopsis of the species of *Henneguya* Thélohan, 1892 (Cnidaria: Myxosporea: Myxobolidae) described since 2012. Systematic Parasitology 100(3): 291–305. https://doi.org/10.1007/s11230-023-10088-2

Sousa FB, Milanin T, Morandini AC, Espinoza LL, Flores-Gonzales A, Gomes ALS, Matoso DA, Mathews PD (2021) Molecular diagnostic based on 18S rDNA and supplemental taxonomic data of the cnidarian coelozoic *Ceratomyxa* (Cnidaria, Myxosporea) and comments on the intraspecific morphological variation. Zoosystematics and Evolution 97(2): 307–314. https://doi.org/10.3897/zse.97.64769